Full Paper

Silicon Micromachined Infrared Thin-Layer Cell for In Situ Spectroelectrochemical Analysis of Aqueous and Nonaqueous Solvent System

Kwang-Seok Yun,*[a] *Segyeong Joo*,[b] *Hong-Jeong Kim*,[c] *Juhyoun Kwak*,[c] *Euisik Yoon*[a]

[a] Department of Electrical Engineering and Computer Science (Division of Electrical Eng.), Korea Advanced Institute of Science and Technology (KAIST), 373-1 Guseong-dong, Yuseong-gu, Daejeon 305-701, Korea
*e-mail: ksyun@iml.kaist.ac.kr
[b] Department of Biomedical Engineering, Seoul National University, Youngun-dong, Jongro-gu, Seoul 110-744, Korea
[c] Department of Chemistry and School of Molecular Science (BK21), Korea Advanced Institute of Science and Technology (KAIST), 373-1 Guseong-dong, Yuseong-gu, Daejeon 305-701, Korea

Received: August 30, 2004
Accepted: October 8, 2004

Abstract
This article reports in situ FTIR monitoring of electrochemical reactions using a silicon-based thin-layer cell realized by micromachining fabrication technologies. The proposed device contains a silicon micromachined cavity cell integrated with a gold working electrode, a counter electrode, and a Ag/AgCl reference electrode. Electrochemical, spectroscopic, and spectroelectrochemical characteristics of the fabricated cell have been experimentally measured and exhibited a comparable performance to commercialized CaF_2 thin-layer cells. In situ spectroelectrochemical characteristics have been successfully tested for both 2 mM $K_3Fe(CN)_6$ in an aqueous solution and 2 mM ferrocene in a dichloromethane solution using the fabricated thin-layer cell.

Keywords: Thin-layer cell, Spectroelectrochemical analysis, FTIR, MEMS, Electrochemical cell

1. Introduction

Spectroelectrochemistry is a way of coupling spectroscopic and electrochemical methods, which is employed to investigate intermediate products, electrochemical reaction parameters, and the kinetics of the electrode process in a wide variety of organic, inorganic, and biological redox systems [1–21]. Depending on the spectral region of interest, ultraviolet (UV), visible, or infrared (IR) radiation can be used as a light source for optical spectroscopy. In particular, IR spectroscopy is a widely used tool because nearly all molecular species, with the exception of a few homonuclear molecules, absorb IR radiation [9–12]. The most frequently-used technique is absorption spectroscopy. There are two types of absorption spectroscopy: (1) transmission spectroscopy where the measurement is performed using a beam passing through a cell containing sample solutions and (2) reflectance spectroscopy where the beam is reflected from the cell [1].

Typically, thin-layer transmission spectroelectrochemistry uses a thin-layer cell in which the cell height or sample thickness is comparable to or smaller than the diffusion layer of reagents [13–22]. In addition to the benefit of conservation of valuable sample, thin-layer cell is very useful for spectroelectrochemical analysis because the entire solution in thin-layer cell is rapidly and completely electrolyzed and this makes it possible to obtain spectroscopic information without interference of bulk solution [15, 16].

Since the first infrared thin-layer spectroelectrochemical method was reported in 1968 [3], several different designs for optically-transparent IR spectroelectrochemical thin-layer cells have been reported [11–15]. For a nonaqueous solution, NaCl or other salt plates have been used for the optical window, while an external gasket, such as Teflon, was used to form a shallow gap between wall plates. Instead, Niu et al. used carved CaF_2 plates for aqueous and nonaqueous solutions [13]. However, all these previous cells have certain drawbacks: (1) three electrodes must be manually integrated with the plates and this is very tedious and time-consuming work; (2) accurate gap control is difficult; and (3) the cost of carved CaF_2 cell plates is very high.

In this work, we propose a new IR thin-layer cell fabricated with silicon wafers and monolithically integrated working, counter, and reference electrodes using microelectromechanical systems (MEMS) techniques. The proposed thin-layer cell is applied to obtain clear Fourier transform infrared (FTIR) spectra of aqueous and nonaqueous sample solutions.

2. Experimental

2.1. Design of Thin-Layer Cell for In Situ FTIR Monitoring System

In situ FTIR monitoring system performs IR spectroscopy during electrochemical reactions. Electrochemical reaction

  DOI: 10.1002/elan.200403202

is induced by electrical signals imposed on the electrodes located inside the cell from an external electrochemical experimental setup. Infrared radiation passes through the cell including the sample liquid and transmittance is measured to observe specific electrochemical reactions for various wavelengths.

As described in the previous section, a thin-layer cell is an electrochemical cell with a depth comparable to or smaller than the diffusion length of the observed chemical species. A typical thin-layer spectroelectrochemical setup is composed of a few parts including: two IR transmittable plates separated by a small gap forming a thin layer; an optically-transparent working electrode between the two plates; and reference and counter electrodes contacting the solution in the thin-layer. In order to achieve a suitable IR transmittance through the working electrode, a metal micromesh electrode has been utilized in this work [3, 22].

Figure 1 shows the proposed IR thin-layer cell. A silicon wafer is used as cell plates, on which a gold mesh working electrode, a gold counter electrode, and a Ag/AgCl reference electrode are fully integrated. A thin-layer cavity region is formed by silicon anisotropic etching. It can be assumed that silicon does not absorb IR since the band gap of silicon is basically larger than the energy spectrum of IR signals used in FTIR measurement systems. Figure 2 shows the FTIR response of bulk CaF_2 wafers compared with that of a double-side polished silicon wafer with a 100 μm-etched cavity. The initial silicon wafer thickness is about 500 μm. Therefore, the actual silicon layer exposed to IR absorption is about 400 μm. The transmittance of a silicon wafer is about 50% smaller than that of a bulk CaF_2 wafer due to the air/silicon and silicon/air reflection at the interface. In spite of the decrease in transmittance, the IR transmittance of silicon is very uniform in the wide range of the measured IR spectrum. This means that silicon can be used to detect characteristic absorption peaks and monitor the IR spectrum of certain chemical reactions without any interference

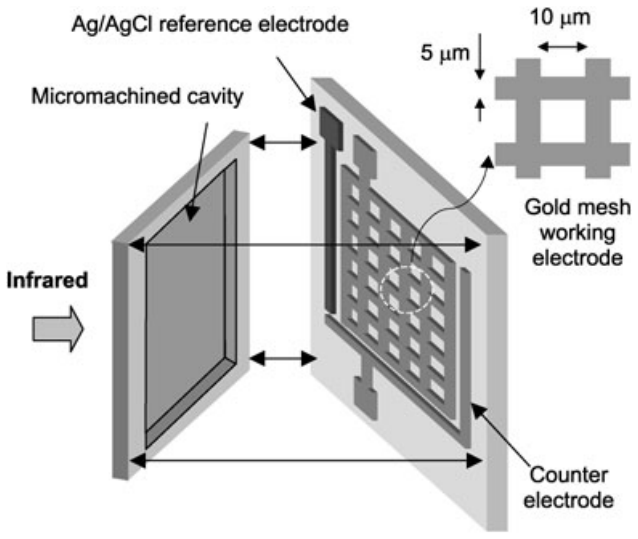

Fig. 1. Proposed structure of micromachined IR thin-layer cell.

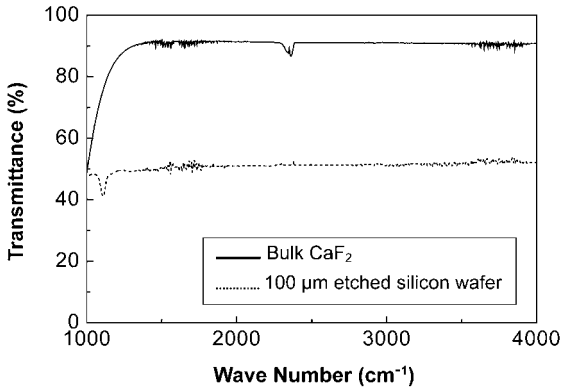

Fig. 2. FTIR transmittance of bulk CaF_2 plates compared with that of a double-side polished silicon wafer with a 100 μm-etched cavity.

in absorption signals. In the current study, the cavity depth was fixed at 100 μm and the gold mesh lines and spaces at 5 μm and 10 μm, respectively.

2.2. Fabrication of Thin-Layer Cell

As described in Figure 1, the proposed thin-layer cell is composed of two silicon plates which are combined together to form a thin-layer cell. One is the bottom plate which contains three electrodes; and the other is the cover plate on which a micromachined cavity is formed.

Figure 3 shows the fabrication process for each silicon plates and schematic view of thin-layer formation. A (100) double-side polished silicon wafer is used to minimize any IR interference on the surface. For a cover plate, thermal oxide is grown on both sides of the silicon wafer in a high temperature furnace (Figure 3a). Next, a photoresist is spin-coated and selectively exposed to ultraviolet (UV) light using glass photomask that allows UV light to strike only selected area of photoresist. Then the exposed photoresist is dissolved in developer solution. With this patterned photoresist as an etch mask, the oxide on front side is etched in buffered hydrofluoric acid (BHF) (Figure 3b). After removal of the photoresist on entire area by using acetone, the silicon is etched in a 25% tetramethyl ammonium hydroxide (TMAH) solution to form a cavity (Figure 3c). In this step, the silicon is anisotropically etched with negligible lateral etch rate compared with vertical etch rate that is dependant on a crystal plane orientation. Finally, the entire oxide film is removed (Figure 3d). For a bottom plate, thermal oxide is grown as a first step (Figure 3e). Next, a Cr/Au layer (20/300 nm) is deposited and patterned to define both working and counter electrodes (Figure 3f). Then, a Cr/Ag layer (20/400 nm) is also patterned for reference electrode and the entire oxide layer is etched using the patterned metal film as a mask (Figure 3g). Finally, the Ag layer is oxidized by dipping it in a 25 mM $FeCl_3$ solution for 2 minutes to create a solid-state quasi-reference electrode (Ag/AgCl) (Figure 3h).

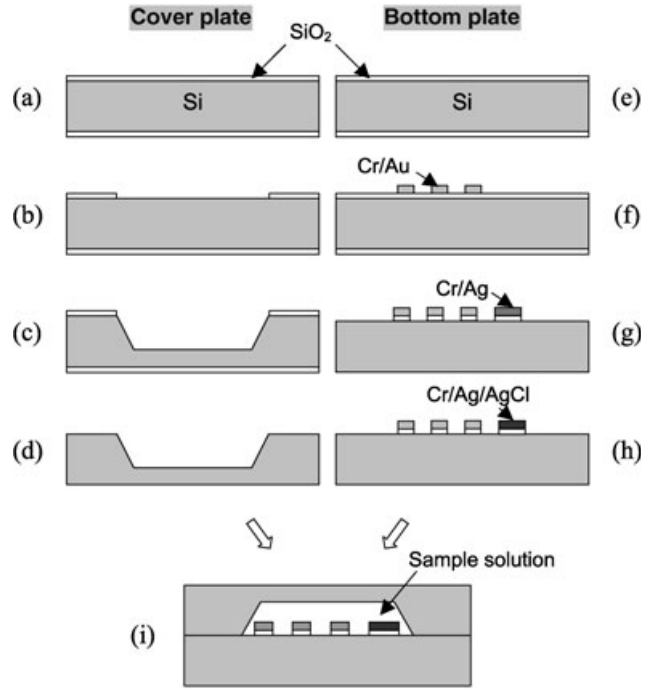

Fig. 3. Fabrication process of cover and bottom plates composing thin-layer cell and schematic view for thin-layer formation.

2.3. Spectroelectrochemical Experiment

After fabricating each part, sample solution is inserted between the two plates and an external jig is used to fix the cell in the FTIR system (Figure 3i). Because of the hydrophobic property of silicon surface, there is no leakage of aqueous solution through the junction between the two plates. In case of nonaqueous solvent, the edge of the thin-layer cell is enclosed by Teflon tape to block the solvent leakage. The three pads on the thin-layer cell are then connected to an external electrochemical measurement system. In the current study, the FTIR spectra were measured using a Paragon 500 FTIR spectrometer (Perkin Elmer Inc.) with BAS 100B (Bioanalytical Systems Inc.) for controlling electrochemical reaction.

3. Results and Discussion

Figure 4 shows the fabricated bottom electrode. The gold mesh electrode was formed on 0.9 cm × 0.8 cm area with 5 μm and 10 μm of lines and spaces, respectively. The gold counter electrode and Ag/AgCl reference electrode with a width of 50 μm are located at outer sides of working electrode.

3.1. Reference Electrode Test

To test the fabricated quasi-reference electrode, the potential difference between a commercial reference electrode and the fabricated reference electrode was measured for various hydrochloric acid concentrations. Figure 5 shows the potential difference between the fabricated Ag/AgCl electrode and a commercial Ag/AgCl (dipped in 3 M NaCl solution) reference electrode as a function of various Cl^- concentrations. The Figure shows that the fabricated Ag/AgCl electrode has linear characteristics with a slope of about − 53 mV/dec, which agrees well with a theoretical value of − 58.5 mV/dec. From this, we have confirmed that the fabricated Ag/AgCl electrode can be reliably used as a reference electrode in a solution with a fixed concentration of Cl^- ions.

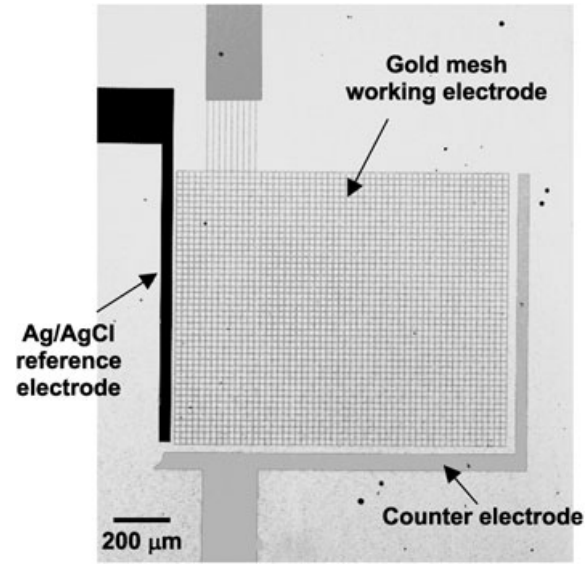

Fig. 4. Microscopic picture of the fabricated bottom plate with working, counter, and reference electrodes.

3.2. Cyclic Voltammetry of Microelectrodes

Both bulk-like properties as well as thin-layer properties of the electrodes have been evaluated using cyclic voltamme-

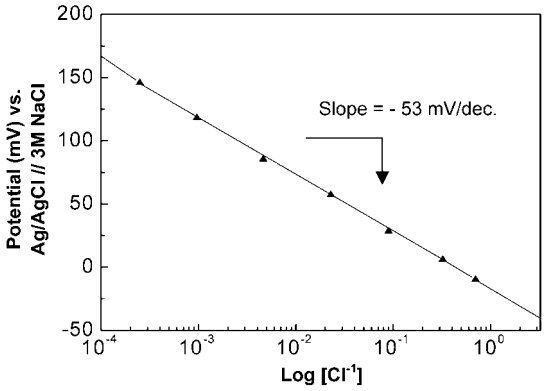

Fig. 5. Measured potential difference between the fabricated Ag/AgCl electrode and a commercial Ag/AgCl (dipped in 3 M NaCl solution) reference electrode as a function of various Cl^- concentrations.

try (CV). Figure 6 presents the cyclic voltammogram measured using a 2 mM $K_3Fe(CN)_6$ solution with 0.1 M KCl as a supporting electrolyte at a scan rate of 2.0 mV/s. The reaction equation can be given as follows:

$$Fe\ (CN)_6^{3-} + e^- \rightleftharpoons Fe\ (CN)_6^{4-} \qquad E^0 = +0.36\ V \qquad (1)$$

Figure 6a shows the CV results performed on the fabricated electrodes without a cover plate. It shows a typical bulk-like cyclic voltammogram, which confirms that the fabricated working, counter and reference electrodes are functioning well as they should be. Figure 6b shows the CV results with a cover plate for three different thin-layer cell depths of 50 μm, 100 μm and 150 μm, respectively. As shown in this result, peak current increases approximately proportional to the cell depth. This implies that the fabricated device operates as a thin layer cell. In this case, cell thickness is much smaller than diffusion length. Therefore, it is not a diffusion-limited process, making the whole solution participate in reaction. Also, it should be noted that in the case of thin-layer electrochemistry (Figure 6b), the current rapidly dropped to nearly zero at higher potentials, while it reaches a certain finite value for the bulk CV as shown in general semi-infinite diffusion condition (Figure 6a).

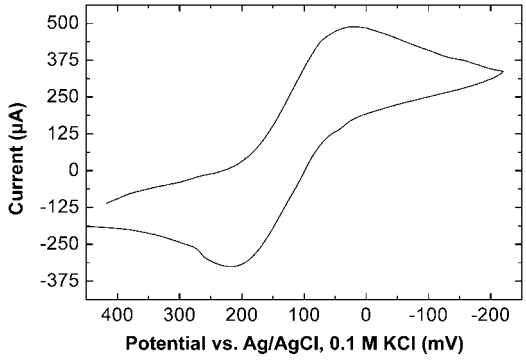

(a)

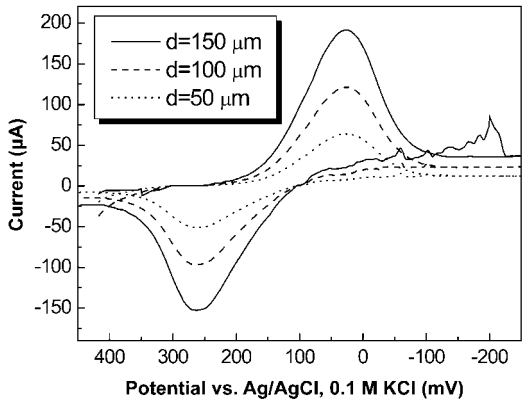

(b)

Fig. 6. Cyclic voltammogram: a) Bulk-like response using the fabricated electrodes without a cover plate, and b) Thin-layer cell response measured for the complete cell integrated with a cover plate for different cavity depths.

Another unique characteristic of thin-layer electrochemistry is peak separation. This means the difference between two potentials where the oxidation and reduction currents are maximal. In theory, there should be no peak separation in thin-layer cyclic voltammogram. However, in practical cases, little peak separation occurs due to uncompensated solution resistance, which causes *iR* drop, from incomplete design of thin-layer cell [23]. As shown in Figure 6b, the peak separation of the fabricated electrochemical cell has been measured about 250 mV. In this experiment, the counter electrode was located on the outer side of the working electrode which induced large solution resistance as well as unevenly distributed *iR* drop between the counter electrode and the working electrode. The resistances of thin-layer cells estimated from the CV experiments (Figure 6b) are about 700 Ω, 1050 Ω and 2040 Ω for the cell thicknesses of 150 μm, 100 μm and 50 μm, respectively. The peak separation may be reduced by closing the space between counter and working electrodes or by slowing the scan rate in the future work.

3.3. FTIR Spectrum of Thin-Layer Cell

Figure 7 compares the FTIR spectrum of the fabricated thin-layer cell with that of a commercial CaF_2 cell for a 2 mM $K_3Fe(CN)_6$ solution. In the case of the fabricated thin-layer cell, the total transmittance is decreased by a factor of about ten due to reflectance at the interface between air and silicon surface. However, the characteristic shape is very distinctive and identical to that of the commercial cell and clearly exhibited the characteristic absorption peak of $Fe(CN)_6^{3-}$ at 2114 cm^{-1} [13].

3.4. In Situ FTIR Spectroelectrochemical Analysis

An example of the application of proposed silicon-based thin layer cell in in situ spectroelectrochemistry for aqueous and nonaqueous solvent is shown in Figure 8. Figure 8a shows the in situ monitoring of spectroelectrochemical

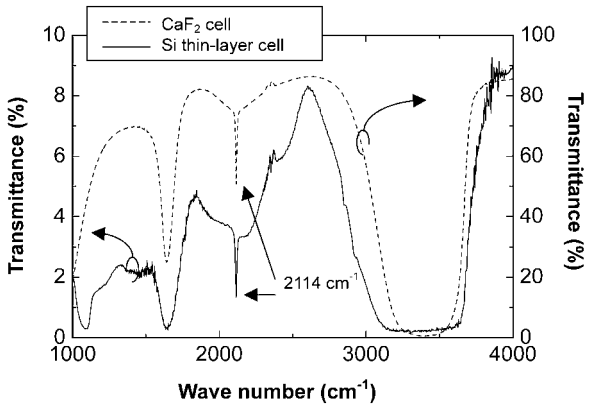

Fig. 7. FTIR spectra of $Fe(CN)_6^{3-}$ in a commercial CaF_2 cell compared with that in the fabricated silicon MEMS thin-layer cell.

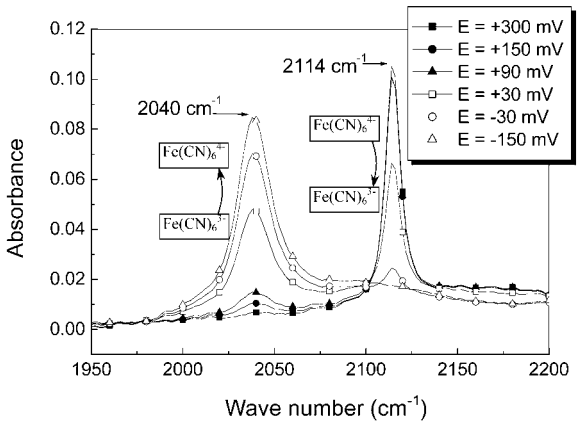

(a)

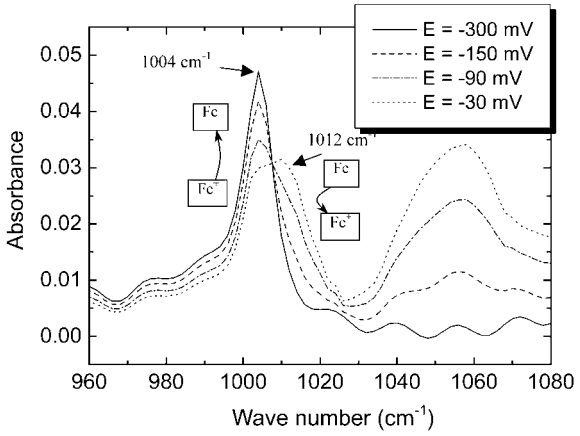

(b)

Fig. 8. a) In situ monitoring of spectroelectrochemical phenomena in 2 mM $Fe(CN)_6^{3-}$ solution with the potential of working electrode changing from 300 mV to −150 mV. b) In situ FTIR spectra of 2 mM ferrocene in dichloromethane solution with varying working electrode potential.

phenomena measured as a function of working electrode potential changes in a 2 mM $Fe(CN)_6^{3-}$ solution. The initial peak was exhibited at 2114 cm^{-1}, which is the characteristic absorption of $Fe(CN)_6^{3-}$. When the potential of the working electrode was decreased, the center metal Fe^{3+} of $Fe(CN)_6^{3-}$ was reduced to Fe^{2+}, thereby increasing the $Fe(CN)_6^{4-}$ peak at 2040 cm^{-1}. When the potential reached −150 mV, the $Fe(CN)_6^{3-}$ was completely reduced to $Fe(CN)_6^{4-}$, which eliminated the peak at 2114 cm^{-1}, leaving a peak only at 2040 cm^{-1}.

We also performed an experiment using a nonaqueous solution in order to investigate the possibility of applications in any solvent system. Figure 8b shows the in situ monitoring of spectroelectrochemical phenomena when using 2 mM ferrocene (C_5H_5–Fe–C_5H_5) in 0.1 M tetrabutylammonium perchlorate/dichloromethane (TBAP/CH_2Cl_2) solution. The characteristic absorption peak of ferrocene at 1004 cm^{-1} decreases with an increase in the working electrode potential. Meanwhile, a new peak for ferricenium ion (C_5H_5–Fe^+–C_5H_5) grows at 1012 cm^{-1}, showing that ferrocene was converted to ferricenium ion by an electrochemical reaction [12]. In this experimental result, we have also observed an increasing peak at 1058 cm^{-1} during the oxidation of ferrocene. We speculate that this broad peak is caused by oxidation of silicon surface near the electrodes and will be clarified in further experiments and analysis [24].

4. Conclusions

A new IR thin-layer cell has been proposed and fabricated using silicon micromachining technology. The fabricated thin-layer cell includes an anisotropically-etched silicon cover plate enclosed on the top of a bottom plate containing a gold mesh working electrode, a gold counter electrode, and a Ag/AgCl solid-state reference electrode. Spectroelectrochemical characteristics of aqueous and nonaqueous sample solutions of 2 mM $K_3Fe(CN)_6$ and 2 mM ferrocene, respectively, have been successfully monitored using the fabricated thin-layer cell. The fabricated MEMS thin-layer cell has exhibited relatively good electrochemical, spectroscopic, and spectroelectrochemical characteristics when compared with commercially-available thin-layer cells. This work has opened a new possibility of enabling low-cost and convenient detection of intermediates or products in chemical redox reactions and accurate identification of reaction mechanisms in chemical redox couples.

5. Acknowledgements

This work has been partially supported by the Intelligent Microsystem Center of 21C New Frontier Project in Korea, KOSEF through the MICROS center at KAIST and Brain Korea 21 Project, the school of information technology, KAIST in 2004.

6. References

[1] W. R. Heineman, *Anal. Chem*. **1978**, *50*, 390A.
[2] A. J. Bard, L. R. Faulkner, *Electrochemical Methods*, Wiley, New York **1980**, ch. 14.
[3] W. R. Heineman, J. N. Burnett, R. W. Murray, *Anal. Chem*. **1968**, *40*, 1974.
[4] M. Petek, T. E. Neal, R. W. Murray, *Anal. Chem*. **1971**, *43*, 1069.
[5] T. Kuwana, *Acc. Chem. Res*. **1976**, 9, 241.
[6] D. E. Albertson, H. N. Blount, F. M. Hawkridge, *Anal. Chem*. **1979**, *51*, 556.
[7] M. D. Porter, S. Dong, Y.-P. Gui, T. Kuwana, *Anal. Chem*. **1984**, *56*, 2263.
[8] S. Dong, Y. Yang, G. Cheng, *J. Electroanal. Chem*. **1992**, *324*, 219.
[9] J. K. Foley, S. Pons, *Anal. Chem*. **1985**, *57*, 945A.
[10] K. M. Kadish, X. H. Mu, X. Q. Lin, *Inorg. Chem*. **1988**, *27*, 1489.
[11] D. L. DuBois, *Inorg. Chem*. **1984**, *23*, 2047.
[12] J. P. Bullock, D. C. Boyd, K. R. Mann, *Inorg. Chem*. **1987**, *26*, 3084.
[13] J. Niu, S. Dong, *Electrochim. Acta* **1995**, *40*, 823.

[14] M. E. Rosa-Montañez, H. D. Jesús-Cardona, C. R. Cabrera-Martínez, *Anal. Chem*. **1998**, *70*, 1007.
[15] D. Moss, E. Naberdryk, J. Breton, W. Mantele, *Eur. J. Biochem.* **1990**, *187*, 565.
[16] A. T. Hubbard, F. C. Anson, *Electroanal. Chem.*, Vol. 4 (Ed: A. J. Bard), Marcel Dekker, New York **1970.**
[17] W. A. Nevin, A. B. P. Lever, *Anal. Chem*. **1988**, *60*, 727.
[18] R. K. Rhodes, K. M. Kadish, *Anal. Chem*. **1981**, *53*, 1539.
[19] J. Zak, M. D. Porter, T. Kuwana, *Anal. Chem*. **1983**, *55*, 2219.
[20] P. A. Mosier-Boss, R. Newbery, S. Szpak, S. H. Lieberman, *Anal. Chem*. **1996**, *68*, 3277.
[21] N. J. Simmons, M. D. Porter, *Anal. Chem*. **1997**, *69*, 2866.
[22] R. W. Murray, W. R. Heineman, G. W. O'Dom, *Anal. Chem*. **1967**, *39*, 1666.
[23] G. M. Tom, A. T. Hubbard, *Anal. Chem*. **1971**, *43*, 671.
[24] T. Morioka, S. Kimura, N. Tsuda, C. Kaito, Y. Saito, C. Koike, *Mon. Not. R. Astron. Soc.* **1998**, *299*, 78.